ORIGINAL RESEARCH

A Novel Tetramethylpyrazine Chalcone Hybrid-HCTMPPK, as a Potential Anti-Lung Cancer Agent by Downregulating MELK

Yan Ma[1,2,]*, Qian Cui[3,]*, Wenjing Zhu[1,4,]*, Mei Wang[1,2], Li Zhai[5], Wenmin Hu[1,2], Dongdong Liu[6], Min Liu[5], Yongchun Li[2], Meng Li[2], Wei Han[1,2]

[1]Qingdao Key Laboratory of Common Diseases, Qingdao Municipal Hospital, School of Medicine and Pharmacy, Ocean University of China, Qingdao, Shandong, 260071, People's Republic of China; [2]Department of Respiratory and Critical Care Medicine, Qingdao Municipal Hospital, University of Health and Rehabilitation Sciences, Qingdao, 266071, People's Republic of China; [3]Department of Respiratory and Critical Care Medicine, Shenzhen Luohu People's Hospital, Shenzhen, 518000, People's Republic of China; [4]NMPA Key Laboratory for Quality Research and Evaluation of Traditional Marine Chinese Medicine, Qingdao, 266071, People's Republic of China; [5]Department of Pharmacy, Qingdao Municipal Hospital, University of Health and Rehabilitation Sciences, Qingdao, 266071, People's Republic of China; [6]Department of Respiratory and Critical Care Medicine, Shanting District People's Hospital, Zaozhuang, 277200, People's Republic of China

*These authors contributed equally to this work

Correspondence: Wei Han; Meng Li, Department of Respiratory and Critical Care Medicine, Qingdao Municipal Hospital, University of Health and Rehabilitation Sciences, Qingdao, 266071, People's Republic of China, Email hanw@uor.edu.cn; cqdpd@126.com

Purpose: Lung adenocarcinoma currently ranks the leading causes of cancer-related mortality worldwide. Many anti-inflammation herbs, like tetramethylpyrazine, have shown their anti-tumor potentials. Here, we evaluated the role of a novel chalcone derivative of tetramethylpyrazine ((E) -1- (E) -1- (2-hydroxy-5-chlorophenyl) -3- (3,5,6-trimethylpyrazin-2-yl) -2-propen-1, HCTMPPK) in lung adenocarcinoma.

Methods: The effects of HCTMPPK on cell proliferation, apoptosis, and invasion were investigated by in-vitro assays, including CCK-8, colony formation assay, flow cytometry, transwell assay, and wound-healing assay. The therapeutic potential of HCTMPPK in vivo was evaluated in xenograft mice. To figure out the target molecules of HCTMPPK, a network pharmacology approach and molecular docking studies were employed, and subsequent experiments were conducted to confirm these candidate molecules.

Results: HCTMPPK effectively suppressed the proliferative activity and migration, as well as enhanced the apoptosis of A549 cells in a concentration-dependent manner. Consistent with this, tumor growth was inhibited by HCTMPPK significantly in vivo. Regarding the mechanisms, HCTMPPK down-regulated Bcl-2 and MMP-9 and up-regulating Bax and cleaved-caspase-3. Subsequently, we identified 601 overlapping DEGs from LUAD patients in TCGA and GEO database. Then, 15 hub genes were identified by PPI network and CytoHubba. Finally, MELK was verified to be the HCTMPPK targeted site, through the molecular docking studies and validation experiments.

Conclusion: Overall, our study indicates HCTMPPK as a potential MELK inhibitor and may be a promising candidate for the therapy of lung cancer.

Keywords: HCTMPPK((E) -1- (E) -1- (2-hydroxy-5-chlorophenyl) -3- (3,5,6-trimethylpyrazin-2-yl) -2-propen-1), chalcone, TMP, lung adenocarcinoma, network pharmacology, AutoDock

Introduction

Lung cancer is a highly lethal malignancy globally,[1] with non-small cell lung carcinoma (NSCLC) accounting for approximately 85% of all diagnosed cases. Despite this, the five-year survival rate for NSCLC is merely 15%.[2] Lung adenocarcinoma, which comprises approximately 40% of lung cancers, is the primary cause of morbidity and mortality in this context.[3]

Most patients with lung cancer are typically diagnosed at an advanced or metastatic stage, and the primary therapeutic approach for NSCLC continues to involve a combination of surgical intervention and chemotherapy.[4–7] However, there are still many lung cancer patients who do not have an available immunotherapy regimen, do not have a specific molecular therapeutic target, and cannot tolerate the intense side effects of chemotherapy drugs. The therapeutic needs of these patients have prompted us to look for the development of novel, low-toxicity anticancer drugs from herbs that have some research basis. Therefore, it is crucial to discover new antineoplastic agents that are more selective towards malignant cells and less toxic to normal cells.

The biologically active phytochemicals exhibit hypotoxic and pleiotropic properties, exerting interference on diverse cellular processes associated with the onset and progression of cancer.[8] Numerous natural products derived from herbal medicines exhibit anticancer activities,[9] encompassing anti-proliferative, pro-apoptotic, anti-metastatic, and anti-angiogenic effects.[10] Moreover, they modulate autophagy, reverse multidrug resistance, balance immunity, and enhance chemotherapy both in vitro and in vivo.[11] Notably, chalcone—a natural compound containing αβ-unsaturated carbonyl groups—has emerged as a pivotal pharmacophore with potent tumor-inhibiting effects.[12] Tetramethylpyrazine (ligustrazine, TMP) is an active alkaloid monomer containing potent bioactive constituents. Extensive research has demonstrated the significant inhibitory effects of TMP and its derivatives on various cancer cell lines, including lung cancer cells,[13,14] colorectal cancer,[15] hepatocellular carcinoma,[16] and breast cancer cells.[17] The inhibitory effects are attributed to modulating various biological processes, such as inducing apoptosis. In recent years, the use of TMP in tumor treatment has gained attention; however, its application is significantly hindered by limitations like rapid metabolism and a short half-life. By structurally altering chalcone derivatives, we have synthesized compounds that substantially enhance antitumor activity and prolong the original plant active ingredient's half-life while reducing cytotoxicity and improving selectivity.[12] The hybridization of chalcone fraction with TMP anticancer pharmacophore offers a promising approach for developing novel anticancer drugs,[18,19] overcoming drug resistance and providing higher activity and enhanced specificity.[20]

To improve the shortcomings of TMP with fast metabolism and short half-life, we added the pyrazine ring structure of TMP based on chalcone parent nucleus and designed a new compound (E)-1-(E)-1-(2-hydroxy-5-chlorophenyl)-3-(3,5,6-3-methylpyrazin-2-yl)-2-toluene-1 (HCTMPPK) based on the principle of hybridization and electron isomerization (Figure 1) in our previous research.[21] Our study investigates the effects of HCTMPPK on lung adenocarcinoma cells to clarify its role in suppressing this type of cancer and identify potential downstream molecules and pathways through network pharmacology. These findings may provide new drugs for treating lung adenocarcinoma.

Maternal embryonic leucine zipper kinase (MELK) is involved in the development of numerous cancers, and is considered a novel oncogene. Multiple studies have demonstrated that MELK is overexpressed in a wide range of cancers, and its elevated expression is associated with a poor prognosis.[22–25] A diverse range of protein substrates have been identified to interact with MELK and regulate its activity through phosphorylation-dependent mechanisms. Activation of MELK is triggered by various stress stimuli, which subsequently promote the activation of apoptosis signal-regulated kinase 1 (ASK1),[26] transforming growth factor-β (TGF-β)[27] and p53 signaling pathways.[26] Activated MELK plays a role in regulating numerous cellular functions, including cell proliferation, cell cycle arrest, spliceosome assembly, stem cell self-renewal, metabolism, and apoptosis.[28,29] In lung cancer, it has been demonstrated that the overexpression of MELK stimulates the proliferation and metastasis of LUAD cells. Additionally, MELK mediates the metastasis of LUAD cells by regulating the expression of Slug, Twist1, MMP7, N-catenin, and E-catenin. It also
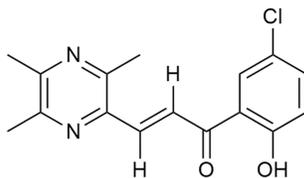

Figure 1 Compound HCTMPPK (E)-1-(E)-1-(2-hydroxy-5-chlorophenyl)-3-(3,5,6-3-methylpyrazin-2-yl)-2-toluene-1.

regulates the G2/M phase through the PLK1-CDC25C-CDK1 pathway and plays a role in inhibiting cellular apoptosis and pyroptosis.[30]

Materials and Methods

Cell Culture

Human lung adenocarcinoma cell line (A549) and human normal lung bronchial epithelial cells (BASE-2B) were obtained from CAS. BASE-2B, A549 cells were cultivated in RPMI-1640 medium (Hyclone, Thermo Scientific, USA) supplemented with 10% fetal bovine serum (FBS, BI, Shanghai, China) and 1% penicillin-streptomycin (Solarbio, Shanghai, China). The cells were incubated in a humidified incubator with 5% CO_2 at 37 °C.

Drug Solution Preparation

The compound HCTMPPK used in the study was synthetized by Zou Jin-mi of Professor Liu Xin-yong research group of Shandong University. HCTMPPK powder was dissolved in DMSO to make a stock solution, and an appropriate amount of stock solution was prepared with complete medium to a high concentration solution of 1000 μmol/L and diluted to a concentration of 2.5, 5, 7.5, 12.5 and 15 μmol/L of drug-containing medium. Animals were injected intraperitoneally with the drug at the solvent ratio of DMSO: PEG 400: Saline = 2:30:68.

Cell Counting Kit-8 Assay

Cell viability of human lung adenocarcinoma cell line and human normal lung bronchial epithelial cells (A549 and BASE-2B) were detected by a cell counting kit-8 (CCK-8) assay (TargetMol, USA). Cells were seeded on 96-well plates (2×10^3 cells/well) and cultivated with various concentrations of HCTMPPK for 24 h. And then 10 μL of CCK-8 reagent was added according to the manufacturer's instructions. Finally, the absorbance of each well was measured at 450 nm using a microplate reader (Thermo Scientific, Multiskan Sky) after 1–2 h. Three independent experiments were repeated to get the mean value.

Colony Formation Assay

A549 cells were seeded into the 6-well plates (1000 cells/well) and treated with increasing concentration of HCTMPPK solution. After the incubation period (24h), cells were washed twice with warm PBS (phosphate-buffered saline), and incubated with culture medium for 14 days. The cells were then fixed with cold 4% paraformaldehyde and stained with 0.5% crystal violet to visualize and count number of colonies.

Transwell Assay

Cell invasion was assessed using Invasion Chambers with 8 μm inserts in 24-well plates (Corning, USA). Cells were seeded in the upper chamber and cultured in a serum-free medium, and the lower chamber was supplemented with 15% serum medium. After 24 h of cell incubation, cells on the upper surface were swabbed off, followed by fixing, staining, washing the cells on the lower surface, and photographed for counting.

Wound-Healing Scratch Assay

Cells were seeded onto a six-well plate one day in advance. Cells were scratched using a 200 μL pipette tip, and the cells were incubated in a serum-free medium for 72 h. Scratch wounds were monitored and photographed at 0, 24, 48, and 72 h. Wound closure was imaged and quantified using Image J software.

Flow Cytometry

Cells treated with the indicated concentration of HCTMPPK were collected and the apoptosis rate was detected using an Annexin V-FITC/PI apoptosis detection kit (KeyGEN BioTECH, Jiangsu, China). Cells were resuspended with 500 μL of 1×Binding Buffer, 5 μL of Annexin V-FITC and 5 μL of Propidium Iodide were added and mixed well. The cells were protected from light for 5–10 min at room temperature and assayed using flow cytometry (Beckman Coulter FC500,

USA) within 1 h. The experiment was repeated three times and the apoptosis rate was finally analyzed by FlowJo 10 software.

Western Blotting Assay

The protein was extracted using RIPA Lysis Buffer (Solarbio, Shanghai, China) and the concentration was determined using the BCA protein assay kit (Solarbio, Shanghai, China) according to the instructions. Proteins were separated using SDS-PAGE (8–12% gel). The membrane was blocked with 5% non-fat milk and incubated with primary antibodies at 4 °C overnight. The membranes were incubated with appropriate secondary antibodies (bioss, Beijing, China) at room temperature for 1–2 h. The proteins were visualized by an enhanced chemiluminescence (ECL) system (Millipore, USA) and the SuperSignal West Femto Chemiluminescent Substrate Detection System (Thermo Fischer Scientific, Rockford, IL). The relative protein levels were measured using Image J software, and normalized to Tubulin. Primary antibodies were purchased from Abcam (Abcam, Cambridge, USA) including Bax (ab32503), Bcl-2 (ab182858), Caspase-3 (ab184787), MMP-9 (ab76003), and Tublin were purchased from Elabscience (Elabscience, Wuhan, China).

Quantitative Real-Time PCR Assay

Total RNA was extracted from A549 cells using TRIzol reagent (Invitrogen, Carlsbad, CA, USA) and cDNA was synthesized using ReverTra Ace qPCR RT Master Mix (Toyobo, Tokyo, Japan) according to the manufacturer's instructions. qRT-PCR was conducted in triplicate using SYBR Premix Ex Taq™ (Takara Bio, Inc., Otsu, Japan). See Table S1 for specific primer sequences. The SYBR green gene expression assays were used for PCR amplification by using QuantStudio 3 Flex real-time PCR system from Applied Biosystems. The data were normalized to the internal reference gene GAPDH. The relative expression of the target gene was calculated using the comparative 2-ΔΔCt method.

Tumor Xenograft in Nude Mice

Male thymus-free nude mice (nu / nu, 4–6 weeks) without specific pathogens were purchased from Pengyue (Jinan, China). A549 cells in logarithmic growth state were collected, and were resuspended with serum-free RPMI-1640. Subcutaneously, cells were injected (1×10^7 cells/100μL/per mouse) into the right anterior axilla of mice. Two weeks later, select tumor-bearing mice with tumor volumes ranging from 200mm^3 to 300mm^3, and randomly divide them into two groups of 8 mice each: one group injected with vehicle (physiological saline containing 2% DMSO and 30% PEG400), and the other group injected with HCTMPPK (15 mg/kg, dissolved in the same vehicle as the model group) intraperitoneally (ip) every day for 2 weeks before being euthanized. Monitor tumor growth every other day. Tumor volume (mm^3) was measured using calipers and the standard formula: (length × width^2) × 0.5. Experimental animal procedures were approved by the Animal Ethics Committee of Qingdao Municipal Hospital.

Immunohistochemistry Staining

Formalin-fixed, paraffin embedded tumor sections tissue were dewaxed and rehydrated. Antigen retrieval was performed using sodium citrate (pH=6) for Caspase-3 (Abcam, USA, ab184787), and EDTA (pH=9) for Ki-67 (Proteintech, Wuhan, China) and MELK (Proteintech, Wuhan, China). After blocking with serum, the primary antibodies were incubated overnight at 4°C and biotinylated anti-rabbit secondary antibodies (ZSGB-BIO, China) were incubated for 1h at 37°C. The immunoreactivity was visualized with DAB and the sections were counterstained with hematoxylin. Immunoreactivity was assessed by light microscopy.

Lung Adenocarcinoma Data Collection and Identification of Aberrantly Expressed Genes in LUAD

The GSE32863 dataset (N=58, T=58) and the LUAD data queue were downloaded from the Gene Expression Omnibus (GEO) database (https://www.ncbi.nlm.nih.gov/geo/) and the Cancer Genome Atlas (TCGA) Data Portal (https://www. cancer.gov/ccg/research/genome-sequencing/tcga) GDC Data Portal, respectively. The data in the above databases are

publicly available for free. The "limma" R package in R software (version 4.2.2) was used to identify differentially expressed genes (DEGs). FDR (q-value) < 0.05 and $\log_2 FC > 1$ were considered statistically significant.

Pathway Enrichment Analysis

Perform Gene Ontology (GO) function and Kyoto Encyclopedia of Genes and Genomes (KEGG) pathway enrichment analysis on the up-regulated and down-regulated DEGs using the "clusterProfiler" package in Bioconductor. Then, the results were visualized using the "ggplot2" package ($P < 0.05$).

Protein–Protein Network Analysis

The cross-DEGs were submit to the STRING database (https://www.string-db.org/) to create the protein-protein interactions (PPI) with a minimum required interaction score of 0.7. Then Cytoscape software (version 3.9.1) was utilized to visualize the regulatory network[26,31] and the plugin of CytoHubba in Cytoscape[32] was performed to identify hub genes in the PPI network based on Degree.

Molecular Docking

Molecular docking is a relatively mature computer aided drug design (CADD) technique for direct structural prediction of compounds.[33] Network pharmacology, on the other hand, as an application of multiple disciplines, can infer biological pathways of interactions through a series of "gene-drug-target-disease" networks.[34] The 3D structure of the target protein was downloaded from the PDB database (https://www.rcsb.org). The water molecules and original ligands were removed from the target proteins by PyMOL, and then the target proteins were imported into AutoDock Tools 1.5.7 for hydrogen addition, charge calculation and non-polar hydrogen combination, and then the results were stored in PDBQT format, and the receptor proteins were all placed inside the docking box and coordinate information was generated. Finally, qvina-w was run for molecular docking, and the results were visualized using PyMOL2.4.

Statistical Analysis

All experiments described above were performed at least 3 times. Data are expressed as the mean of each group ± SEM. Analysis of variance (ANOVA) was performed on HCTMPPK data versus controls using GraphPad Prism 5.0 software. The level of significance was set at $P < 0.05$. More details are available in the Supplementary Material.

Result

HCTMPPK Inhibits the Proliferation of A549 Cells

In this study, we initially assessed the toxic effects of HCTMPPK on normal and lung adenocarcinoma cells, respectively, by measuring A549 and BEAS-2B cells survival with CCK-8. HCTMPPK significantly inhibited the viability of A549 cells in a concentration-dependent manner, and in addition, HCTMPPK was less cytotoxic to human normal lung epithelial cells (BEAS-2B) than to A549 cells (Figure 2A, Figure S1), indicating that it was more targeted to A549 cells. The 24-hour HCTMPPK average IC50 profiles against A549 and BEAS-2B cell lines were 18.02 μM and 19.01 μM, respectively (Figure S2). To further investigate the anti-proliferative ability of HCTMPPK on A549 cells, we performed the colony formation assay and observed that HCTMPPK inhibited the proliferation of A549 cells in a concentration-dependent manner (Figure 2B–C).

HCTMPPK Promotes Apoptosis in A549 Cells

To determine that HCTMPPK inhibited the proliferation of LUAD cells and its cytotoxicity acts in part through the process of apoptosis, the rate of apoptosis in A549 cells after 24 h of administration was measured using Annexin V-FITC/PI double-staining and analyzed by flow cytometry. As shown in Figure 3A, the apoptosis rate of A549 cells exposed to HCTMPPK for 24 h increased in a concentration-dependent manner. As the drug concentration increased, the percentage of early apoptosis was relatively lower and the percentage of late apoptosis increased. These results suggested that HCTMPPK may partly be responsible for the death of LUAD cells in part through the induction of apoptosis.
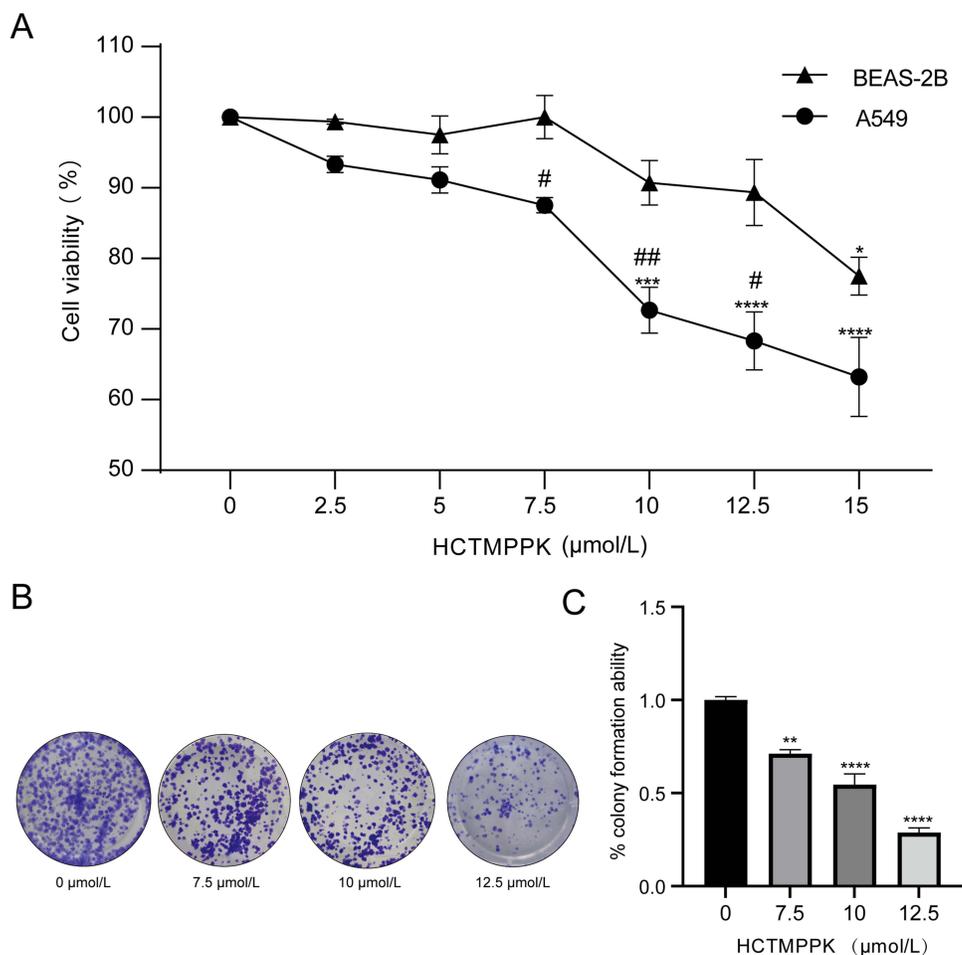
Figure 2 HCTMPPK inhibits the proliferation of lung adenocarcinoma cells. (**A**) Results of CCK-8 assays indicated that HCTMPPK inhibits the proliferation of A549 rather than BEAS-2B. (**B**) Representative pictures of Colony-forming assay. (**C**) The statistical graph of the clone formation experiment. *$P < 0.05$, **$P < 0.01$, ***$P < 0.001$, ****$P < 0.0001$, compared with group 0, #$P<0.05$, ##$P<0.01$, compared with BEAS-2B.CCK-8, cell count kit 8.

In addition, Bax, Bcl-2 and Caspase-3 all play important roles in apoptosis, and in view of this, we investigated the expression levels of several of these apoptosis-related proteins after 24 h of HCTMPPK stimulation. We observed that Bax/Bcl-2 was elevated at the protein level in the administered group of cells after 24 h exposure to different concentrations of HCTMPPK compared to the vector-treated cells (Figure 3B), while the expression of cleaved caspase-3 was enhanced (Figure 3C), which implies that drug treatment promoted apoptosis. Overall, HCTMPPK could lead to cell death through promoting apoptosis of A549 cells.

HCTMPPK Inhibits the Migration of A549 Cells

In addition to its pro-apoptotic effect on A549 cells, our study aimed to investigate the impact of HCTMPPK on the migratory capacity of tumor cells. The results of transwell assay in HCTMPPK groups at different concentrations (7.5, 10, 12.5 μmol/L) showed that the cell migration number was significantly lower than that of the control group after 24 h, and the differences were statistically significant at 10 μmol/L and 12.5 μmol/L concentrations compared with the vector-treated group (Figure 4A). Meanwhile, we also performed wound-healing scratch assays under the same drug stimulation in transwell (Figure 4B), and the results showed that HCTMPPK could inhibit the migration of A549 cells. Further, we used Western blot to further determine the expression level of MMP-9, a protein associated with the invasion process. The results in Figure 4C showed that the expression level of MMP-9 protein was significantly reduced at 10 μmol/L and 12.5 μmol/L compared with the control group, which showed that HCTMPPK could inhibitory effect on the invasion of A549 cells. In conclusion, HCTMPPK can promote apoptosis and inhibit proliferation and invasion of LUAD cells.
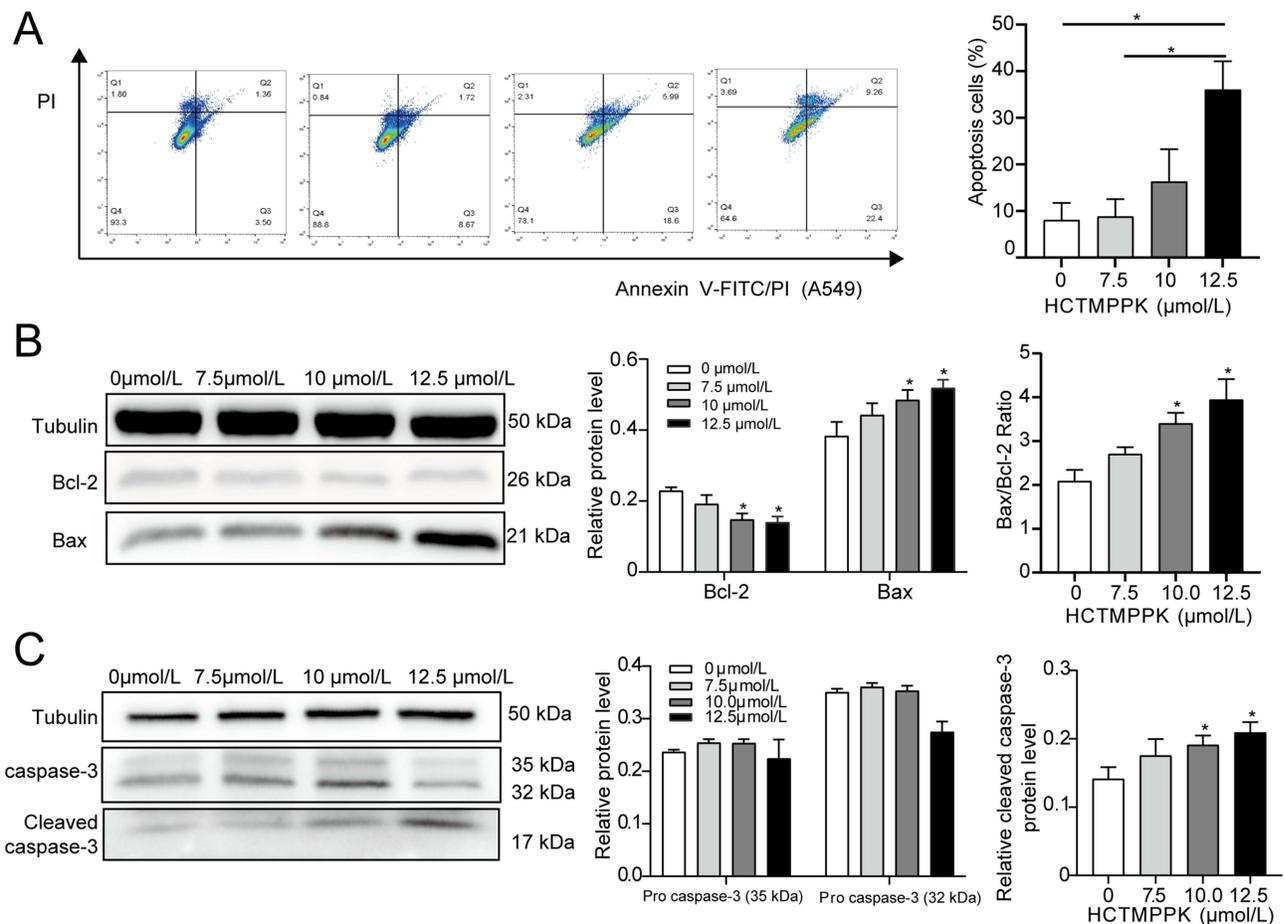
Figure 3 HCTMPPK promotes apoptosis in A549 cells. (**A**) Annexin V-FITC/PI dual staining apoptosis analysis of A549 cells in each group. (**B**) Representative Western blotting and quantification of Bax, Bcl-2. (**C**) Representative Western blotting and quantification of pro caspase-3 and cleaved caspase-3. *$P < 0.05$, *t*-test.

HCTMPPK Inhibits the Growth of A549 Xenograft Tumors in vivo

Based on these results, the present study further evaluated the anti-tumor effects of HCTMPPK in vivo. Firstly, we conducted a long-term toxicity test in mice by continuous administration (0, 15, 30 mg/kg) for 21 days, and the results showed that the dose of 15 mg/kg did not show hepatic and renal toxicity in C57BL/c mice (Table S2, Figure S3), thus we used 15 mg/kg for the subsequent animal experiments. We established a xenograft model in nude mice and grouped tumor-bearing mice with tumor volume greater than 200 mm³ 14 days after subcutaneous inoculation of A549 cells, and treated them with vehicle and HCTMPPK (15 mg/kg) by intraperitoneal injection for 14 days, respectively. Tumor volumes were measured daily from the beginning of treatment. Compared with the model group, the inhibition rate of xenograft tumor size in mice in the HCTMPPK group by intraperitoneal injection was 52% at 14 days of treatment, and a significant difference in the size of transplanted tumors in mice in the drug-treated group compared with the vector control group was observed from day 9 after the start of drug administration (Figure 5A). The tumor masses were weighed after autopsy. The mean volume and weight of tumors in the drug-administered group were significantly lower compared to the control group (Figure 5B). We then assessed the expression levels of Caspase-3 and Ki-67 in the tumor tissues by immunohistochemistry and quantified the immunohistochemical results using FIJI Image J (Figure 5C). The results showed that Ki-67, a marker of cell proliferation, was significantly downregulated by HCTMPPK and Caspase-3, a marker of apoptosis, was significantly upregulated in the tumor tissues. In short, HCTMPPK inhibited the proliferation of lung adenocarcinoma cells and promoted their apoptosis, thus achieving the effect of tumor growth inhibition.
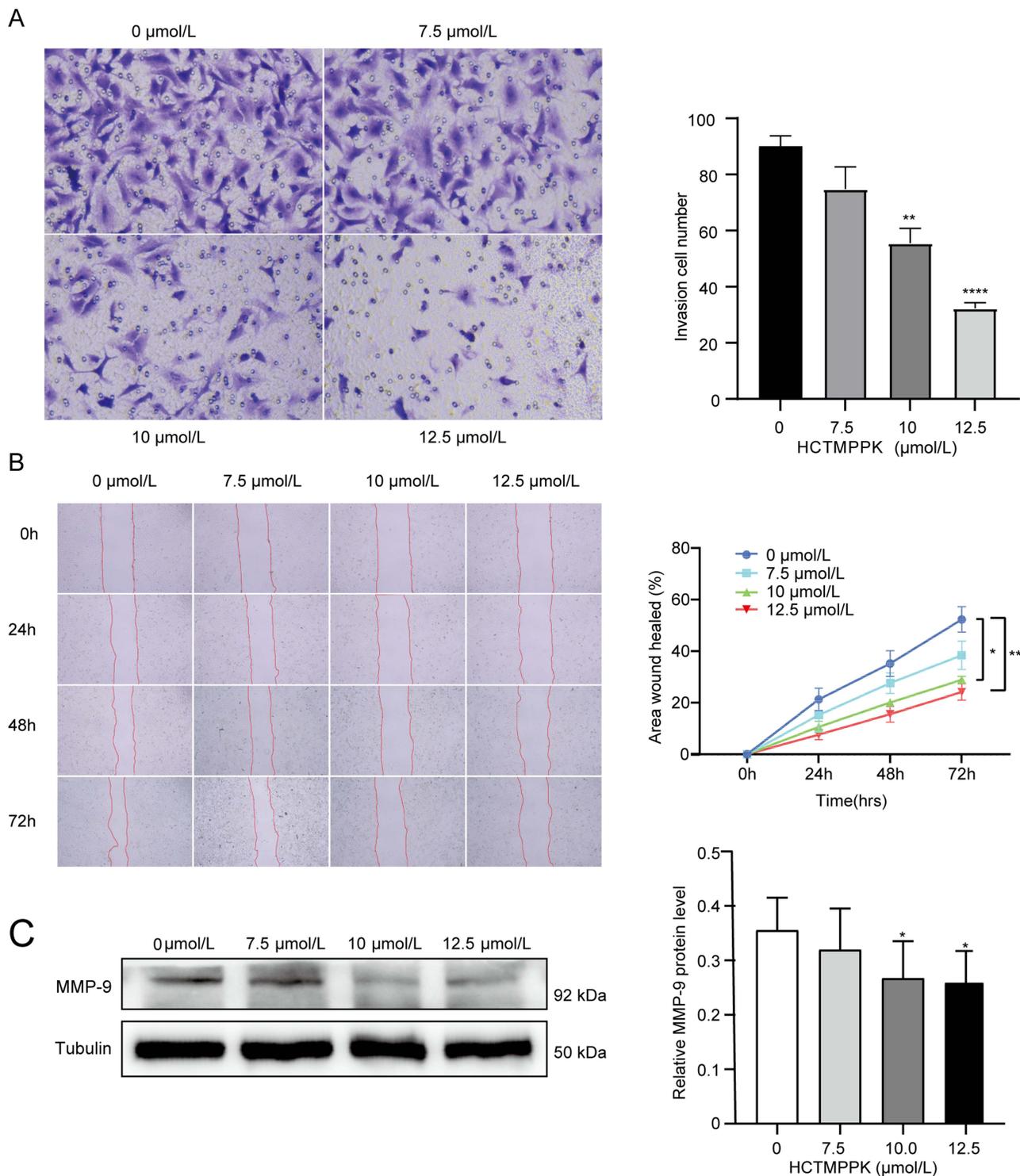
Figure 4 HCTMPPK inhibits the migration of A549 cells. (**A**) Representative pictures of transwell assay and number of migrating cells. (**B**) Wound healing experiments and quantitative chart. (**C**) Representative Western blotting and quantification of the expression of MMP-9 decreased after 24 h exposure to HCTMPPK. *$P < 0.05$, **$P < 0.01$, ****$P < 0.0001$ t-test.

Screening Key Genes for HCTMPPK Interference in LUAD

The raw data in GEO and TCGA were filtered, analyzed, and sorted using the "limma" R package, from which 956 DEGs and 6646 DEGs were extracted, respectively, compared with normal tissues. The "ggplot2"and "pheatmap" packages of
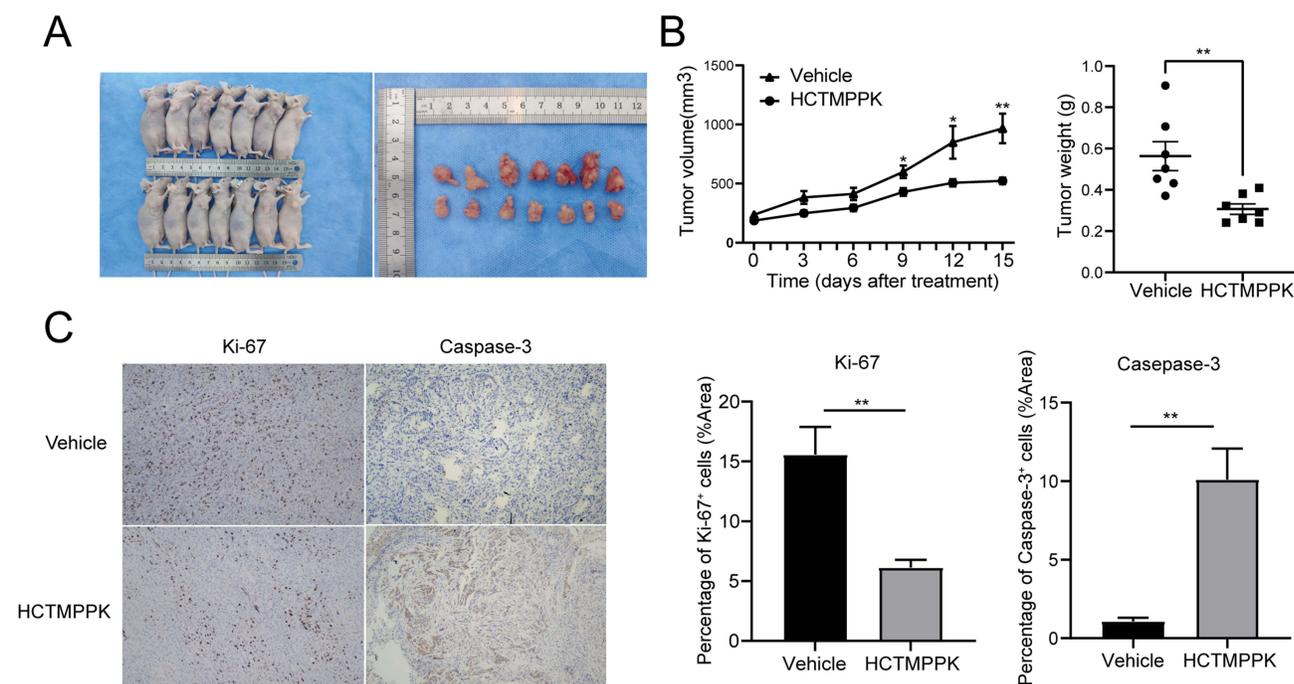
Figure 5 HCTMPPK inhibits the growth of A549 xenograft tumors in vivo. (**A**) Images from subcutaneous xenograft of nude mice and tumors that were harvested in day 15. (**B**) Results showed that the tumor volume and tumor weight in group HCTMPPK were significantly decreased compered to group vehicle. (**C**) Immunohistochemical staining of Ki-67 and Caspase-3 in tumor tissue sections. *$P < 0.05$, **$P < 0.01$, *t*-test.

R software were used to draw heatmap and volcano plot (Figure S4). For conducting more objective and accurate data analysis, 601 overlapped DEGs (ol-DEGs) were detected in GEO and TCGA (Figure 6A and B).

To further explore the specific mechanism of HCTMPPK in exerting pharmacological effects, firstly GO functional and KEGG pathway enrichment analyses were performed. 815 pathways were obtained from GO functional enrichment results, and the top 10 significantly enriched terms in BP, MF and CC categories were plotted separately using the "clusterProfiler" package (Figure 6C and D). The GO analysis of DEGs was mainly related to extracellular matrix organization, cell-matrix adhesion process. The enrichment results of KEGG pathways showed enriched signaling pathways, mainly including Complement and coagulation cascades and Leukocyte transendothelial migration. Among them, the extracellular matrix organization, cell-matrix adhesion process is closely related to tumor development. The PPI network of differentially expressed proteins in LUAD patients in the GEO and TCGA databases was obtained from STRING (Figure 6E and G). The topological parameters of the PPI network were calculated by Cytoscape. The CytoHubba plug-in was used to select the top 15 genes ranked by the MCC method as hub genes, including: MELK, AURKA, JUN, CENPF, TYROBP, AURKB, CCNB2, CDC20, TPX2, ASPM, KIF20A, UBE2C, TOP2A, MMP9 and IL6.

HCTMPPK Inhibits Lung Cancer Progression Through MELK

Next, we predicted the potential targets of HCTMPPK action in lung adenocarcinoma cells. Based on the degrees of common targets in the PPI network and the KEGG results, key lung adenocarcinoma -related targets (eg, AURKA, MELK, JUN) were selected for molecular docking using QuickVina-W (Figure 7A, C and E). The docking results showed that HCTMPPK could bind to the docking pocket with good docking activity with the target proteins. The specific binding modes of target proteins and components were processed and optimized using PyMoL2.4.0. The docking results showed that all the above three target proteins bind well to the HCTMPPK ligand molecule.

The compound HCTMPPK was docked with the proteins AURKA, JUN and MELK respectively. The results (Figure 7A–C) showed that the hydroxyl group on the benzene ring of the compound HCTMPPK forms a hydrogen bond with the amino acid Ala-213 in the cavity of the protein AURKA. The hydroxyl and ketone carbonyl groups of
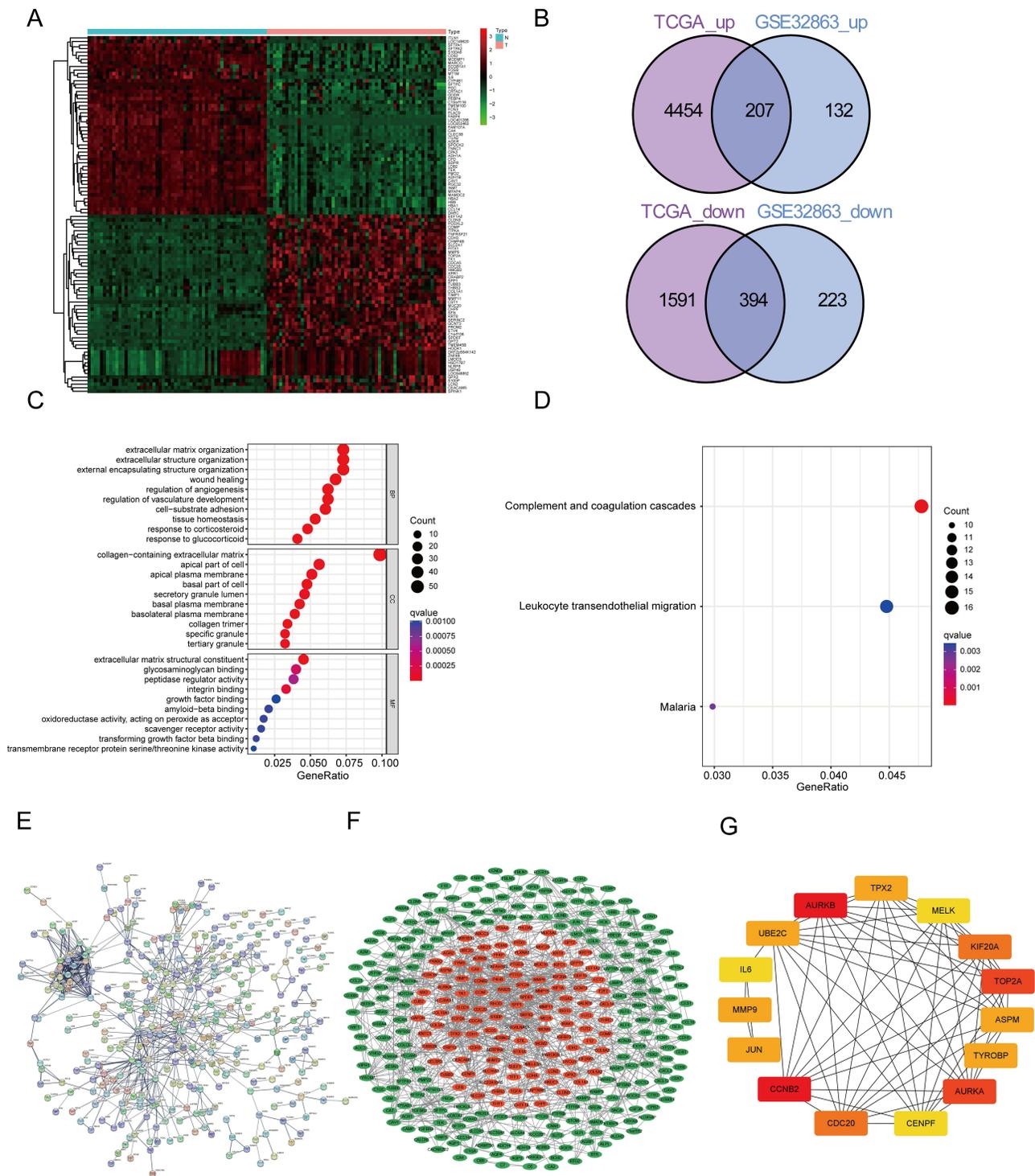
Figure 6 Bioinformatics screening identifies differential genes associated with lung adenocarcinoma. (**A**) Heatmap of up- and down-regulated genes in lung adenocarcinoma patients compared to normal subjects in GEO. (**B**) Wayne's Map of up- and down-regulated genes in lung adenocarcinoma patients compared to normal subjects in TCGA. (**C** and **D**) Bubble plots of GO function and KEGG pathway analysis of crossed DEGs. (**E–G**) PPI network construction and the top 15 hub genes in the PPI network screened based on Degree. In (**F**) red color indicates up-regulated genes and green color indicates down-regulated genes. The darker the node color in (**G**) the higher the score of degree.
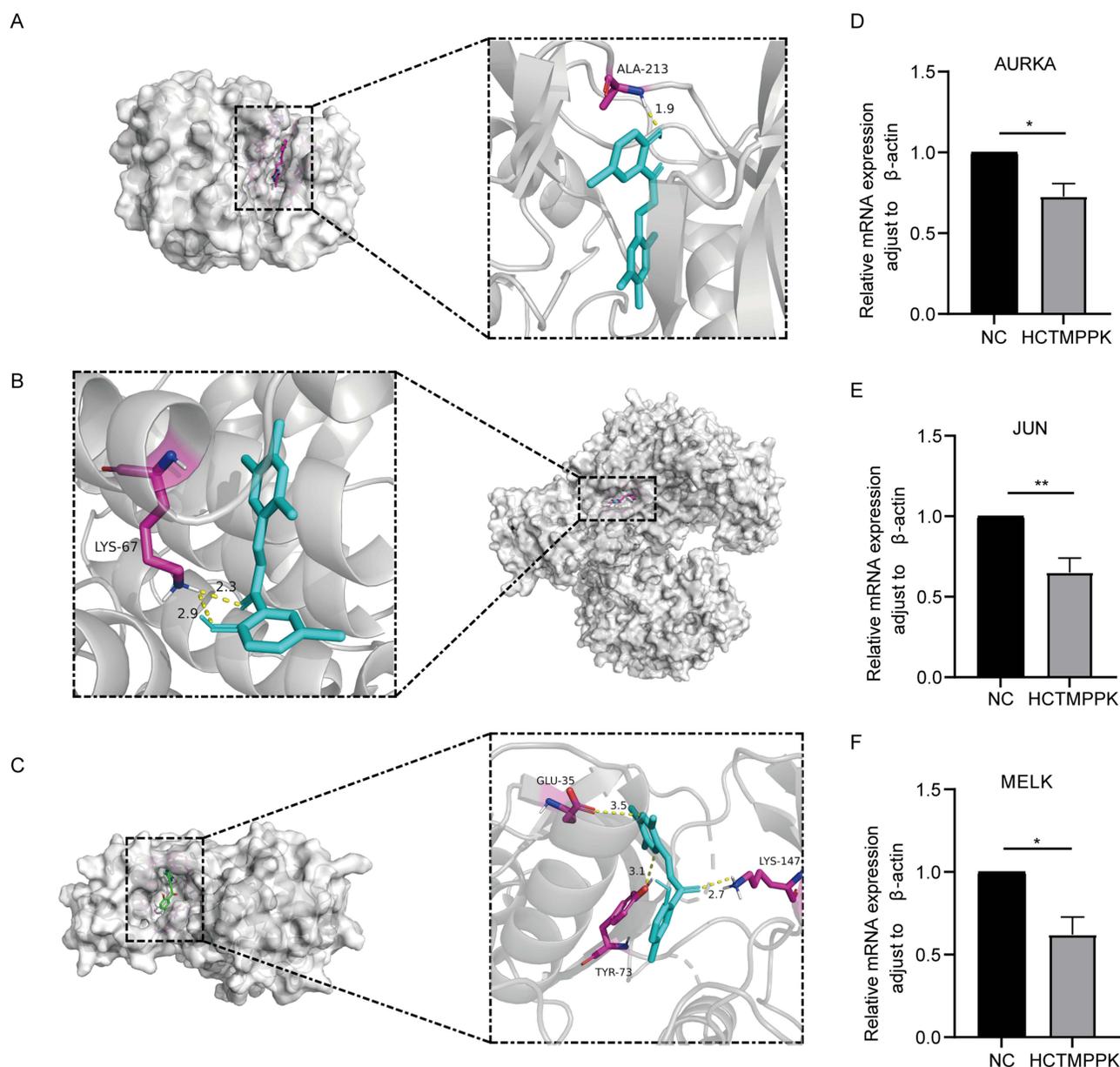
Figure 7 Molecular docking and validation on A549 cells. (**A–C**) In the picture, the cyan part represents the drug molecule, the target protein structures show as white Cartoon Mode. (**D–F**) The rightmost bar graphs indicate the mRNA expression of the corresponding genes in A549 in group NC and HCTMPPK, respectively.; *P < 0.05, **P < 0.01, t-test.

HCTMPPK form hydrogen bonds with the amino acid Lys-67 in protein JUN. The hydroxyl, ketocarbonyl and pyrazine rings of HCTMPPK form hydrogen bonds with the protein MELK and are more stable in the cavity.

To verify the interaction between HCTMPPK and three potential genes, the qPCR was performed on A549 cells after drug administration (Figure 7D–F). Compared with the control group, the expression of JUN, AURKA and MELK genes was significantly reduced after 24 hours, indicating that HCTMPPK could act on these three targets to exert oncogenic effects. To explore the pathway of action of HCTMPPK, we carried out in vivo validation. The qPCR results of tumor tissue that MELK could play a more critical role in the inhibition of the tumorigenesis and development process of HCTMPPK (Figure 8A–C).

Therefore, we further tested the effect of HCTMPPK on MELK expression. In the in vivo experiments, we performed immunohistochemical staining of mouse tumor tissues and quantified the MELK expression-positive regions. The results showed that HCTMPPK resulted in decreased MELK expression (Figure 8D and E). We also did Western bloting on
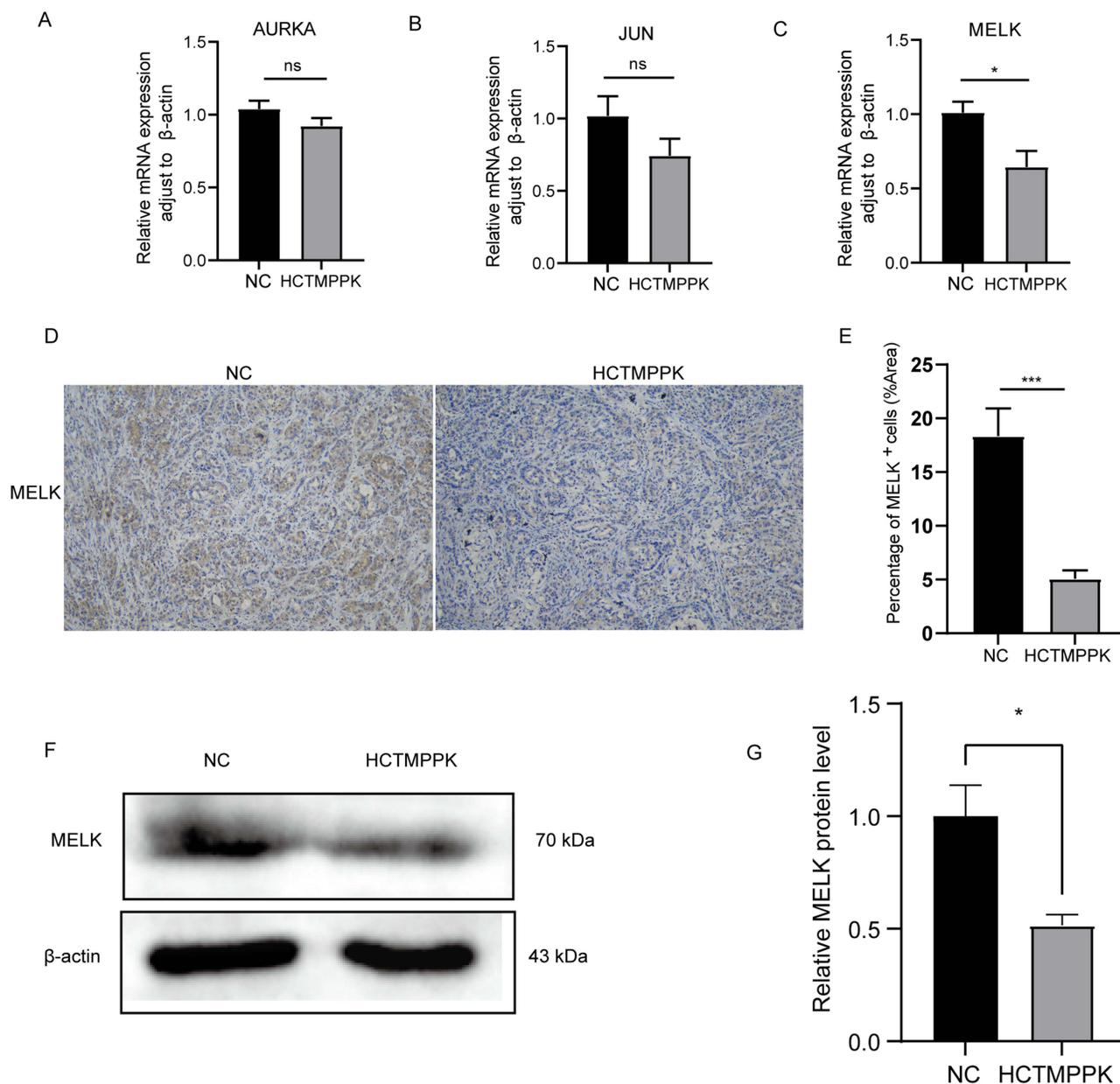
Figure 8 Validation of MELK expression in vitro and in vivo. (**A–C**) The mRNA expressions of AURKA, JUN, and MELK in tumor tissue. (**D–E**) Immunohistochemical staining of MELK in tumor tissue sections and the corresponding quantitative statistic graphs. (**F** and **G**) Representative Western blotting and quantification of MELK in A549. *$P < 0.05$, ***$P < 0.001$, t-test.

A549 cells for verification, and consistent with the IHC results, HCTMPPK downregulated MELK expression in A549 cells (Figure 8F and G).

Discussion

Chemotherapy is a crucial therapeutic modality for solid cancers.[6] Extensive evidence established the apoptosis-promoting effects of chemotherapeutic agents, such as 5-FU, on different tumors, however, their corresponding side effects are significant.[35] The need for less toxic and more effective anticancer drugs for lung cancer patients has led to a search for the development of new antitumor drugs from the rich treasure trove of herbs.

Chalcones represent a significant class of anticancer agents with diverse biological activities, and their hydroxyl derivatives exhibit substantial anti-proliferative effects on cancer cells.[12] TMP alleviates inflammation through inhibiting

TRAF6/c-JUN/NF-κB signaling pathway,[36] enhances antitumor effects,[37] and has also demonstrated its ability to reverse breast cancer by regulating pgp-mediated expression of multidrug resistance in breast cancer cells.[38] In this study, we found that chalcone hybridized with TMP inhibited the growth of A549 cells, induced apoptosis, and showed little cytotoxicity to normal cell lines BEAS-2B.

Previous studies have shown that TMP exerts a dose- and time-dependent inhibitory effect on the proliferation of A549 cells by inhibiting cell cycle progression.[37] HCTMPPK is a hybrid structure comprising of aromatic ketones and enones in conjunction with tetramethylpyrazine, which serves as the central core for diverse biologically significant compounds. A drug is considered to have no significant cytotoxicity if its inhibitory effect on proliferation is below 10%.[39] The results of our CCK-8 assay showed that the safety profile of HCTMPPK in BASE-2B cells within the range of 10–12.5 μmol/L, while significantly inhibiting the proliferative activity of A549 cells. Our plate cloning assay visually depicted the drug's proliferative toxicity on A54 cells as well. This experimental evidence highlights that HCTMPPK exhibits antitumor effects by effectively suppressing lung cancer cell proliferation without inducing significant toxicity in normal cells.

Apoptosis plays a pivotal role in maintaining cellular homeostasis and represents a promising therapeutic target for cancer intervention.[40] Wang et al[41] showed that synthetic TMP-flavonoid derivative compounds induced apoptosis in hepatocellular carcinoma cell line Bel-7402. Then, can the HCTMPPK we studied induce apoptosis in lung cancer cells? In accordance with the findings of Wang et al, our flow results showed that HCTMPPK effectively induced apoptosis in A549 cells, as evidenced by a positive correlation between the drug concentration and the rate of apoptosis (including early and late stages). This suggests that HCTMMPPK can induce cell death through apoptotic pathways. To elucidate the underlying mechanism, Western blotting was employed to assess the levels of Bcl-2 family proteins and caspase family proteins. Bcl-2 forms a heterodimer with Bax when Bcl-2 is highly expressed, which inhibits apoptosis. Therefore, the Bax/Bcl-2 ratio is commonly used to assess the apoptotic status of cells.[42] In the present study, treatment with HCTMPPK resulted in a decrease in Bcl-2 and an increase in Bax expression, leading to apoptosis in A549 cells. This pro-apoptotic property may be attributed to the compound's ability to enhance cysteinase-3 activation while down-regulate Bcl-2 and up-regulate Bax expression.

Migration and invasion are critical processes in the metastasis of pre-cancerous cells.[43] MMP-9, also known as gelatinase B, regulates tumor migration and invasion, and cancer metastasis. Rajasinghe LD[44] found that δ T inhibited MMP-9 activity in a concentration-dependent manner, thereby reducing the migration and invasion of lung cancer cells. In this study, we observed that HCTMPPK downregulates MMP-9 protein expression and inhibits the invasion of A549 cells at concentrations of 10 and 12.5 μmol/L. These findings suggest that HCTMPP has antitumor effects on lung cancer cells. HCTMPPK likely inhibits xenograft through a combination of its pro-apoptotic and anti-invasive/migratory effects tumor growth in mouse models. In our results, HCTMPPK promoted apoptosis of A549 cells and inhibited the migration of A549 cells, so we suggest that HCTMPPK may also inhibit the migration of lung cancer cells by inducing apoptosis. These new findings broaden our understanding of the anticancer pharmacology of HCTMPPK.

In this study, we predicted the interactions between HCTMPPK and its potential protein targets by integrating NSCLC-related information from publicly available databases. Additionally, a docking study was conducted to predict specific interactions between HCTMPPK and its predicted protein targets. Pathway analysis revealed that HCTMPPK regulates cell adhesion and migration processes, which are crucial for the proliferation and metastasis of lung carcinoma. Tumor metastasis is a complex process, with epithelia–mesenchymal transition (EMT) serving as the initial step. Therefore, we further analyzed the proteins associated with these two pathways. The results demonstrated that HCTMPPK can interfere with the progression of NSCLC through multiple targets and pathways. Among these, the top 15 targets included JUN, IL6, TOP2A, MMP9, UBE2C, KIF20A, ASPM, TPX2, CDC20, CCNB2, MELK, AURKB, TYROBP, AURKA, and CENPF.

Absolute values of affinity greater than 4.25 indicate some binding activity, greater than 5.0 indicate good binding activity, and greater than 7.0 indicate strong binding activity.[45] Our molecular docking results showed that the affinity's absolute values of MELK, AURKA, JUN, TOP2, MMP9 were 8.5, 8.4, 7.5, 7.9, 6.5, respectively. Which means HCTMPPK could adapt well to the active regions of MELK and AURKA and regulate their expressions at the transcriptional level. However, during in vivo validation, we observed a significant difference only in MELK.

Furthermore, MELK is an oncogenic kinase essential for metastasis, mitotic progression, and programmed cell death in lung carcinoma. It can enhance the migration and invasion of LUAD by upregulating MMPs, and N-cadherin.[30] Noticeably, the expression of MELK is increased in cancerous tissues, during cell transformation and in mitotically-blocked cells.[46] MELK has indeed been implicated in numerous cellular events in tumorigenesis and malignant progression of human cancers. It achieves this through phosphorylation and regulation of several signaling molecules, including NF-κB[47] and mTOR.[48] Given its significance in these processes, a more detailed exploration of the downstream signaling pathways modulated by MELK in NSCLC is imperative. The current study provides evidence that HCTMPPK influences the developmental process of LUAD by influencing the expression of MELK, suggesting a potential target for therapeutic intervention in lung cancer. Future studies are needed to further elucidate the exact mechanism by which HCTMPPK regulates MELK and its downstream targets in NSCLC.

There are also some limitations in this study. Although we have found that HCTMPPK can inhibit MELK expression, the specific mechanisms remain unclear. Further research could involve labeling HCTMPPK with a fluorescent marker to determine its intracellular location or using immunoprecipitation to identify proteins that directly interact with HCTMPPK.

In conclusion, the HCTMPPK reported in this study could halt or delay the progression of tumor development by inhibiting the proliferation and invasion of lung cancer cells and promoting apoptosis. These findings offer promise for the potential application of chalcone compounds, or their derivatives as effective chemotherapeutic agents based on preclinical principles and molecular basis.

Data Sharing Statement

The datasets used and/or analyzed during the current study are available from the corresponding author on reasonable request.

Ethics Approval and Consent to Participate

All the procedures in this study were approved by the Animal Ethics Committee of Qingdao Municipal Hospital, Qingdao, China (No. 2023-174), and followed the Laboratory animal -Guideline for ethical review of animal welfare of the Ocean University of China.

TCGA and GEO belong to public databases. The patients involved in the database have obtained ethical approval. Users can download relevant data for free for research and publish relevant articles. Thus, the Ethics Committee of Qingdao Municipal Hospital reviewing and waiving the need for ethical approval for the study.

Author Contributions

All authors made a significant contribution to the work reported, whether that is in the conception, study design, execution, acquisition of data, analysis and interpretation, or in all these areas; took part in drafting, revising or critically reviewing the article; gave final approval of the version to be published; have agreed on the journal to which the article has been submitted; and agree to be accountable for all aspects of the work.

Disclosure

The authors report no conflicts of interest in this work.

References

1. Salehi-Rad R, Li R, Paul MK, Dubinett SM, Liu B. The biology of lung cancer: development of more effective methods for prevention, diagnosis, and treatment. *Clin Chest Med*. 2020;41(1):25–38. doi:10.1016/j.ccm.2019.10.003
2. Rafei H, El-Bahesh E, Finianos A, Nassereddine S, Tabbara I. Immune-based therapies for non-small cell lung cancer. *Anticancer Res*. 2017;37 (2):377–387. doi:10.21873/anticanres.11330
3. Lu T, Yang X, Huang Y, et al. Trends in the incidence, treatment, and survival of patients with lung cancer in the last four decades. *Cancer Manag Res*. 2019;11:943–953. doi:10.2147/cmar.S187317
4. Chen P, Liu Y, Wen Y, Zhou C. Non-small cell lung cancer in China. *Cancer Commun*. 2022;42(10):937–970. doi:10.1002/cac2.12359
5. Nagasaka M, Gadgeel SM. Role of chemotherapy and targeted therapy in early-stage non-small cell lung cancer. *Expert Rev Anticancer Ther*. 2018;18(1):63–70. doi:10.1080/14737140.2018.1409624
6. Pirker R. Chemotherapy remains a cornerstone in the treatment of nonsmall cell lung cancer. *Curr Opin Oncol*. 2020;32(1):63–67. doi:10.1097/cco.0000000000000592
7. Wang S, Zimmermann S, Parikh K, Mansfield AS, Adjei AA. Current diagnosis and management of small-cell lung cancer. *Mayo Clin Proc*. 2019;94(8):1599–1622. doi:10.1016/j.mayocp.2019.01.034
8. Constantinescu T, Lungu CN. Anticancer activity of natural and synthetic chalcones. *Int J Mol Sci*. 2021;22(21):11306.
9. Zhai B, Zhang N, Han X, et al. Molecular targets of β-elemene, a herbal extract used in traditional Chinese medicine, and its potential role in cancer therapy: a review. *Biomed Pharmacother*. 2019;114:108812. doi:10.1016/j.biopha.2019.108812
10. Yang A-Y, Liu H-L, Yang Y-F. Study on the mechanism of action of Scutellaria barbata on hepatocellular carcinoma based on network pharmacology and bioinformatics. *Front Pharmacol*. 2022;13:1072547. doi:10.3389/fphar.2022.1072547
11. Luo H, Vong CT, Chen H, et al. Naturally occurring anti-cancer compounds: shining from Chinese herbal medicine. *Chin Med*. 2019;14:48. doi:10.1186/s13020-019-0270-9
12. Ouyang Y, Li J, Chen X, Fu X, Sun S, Wu Q. Chalcone derivatives: role in anticancer therapy. *Biomolecules*. 2021;11(6):894.
13. Dong Y, Yang Y, Wei Y, Gao Y, Jiang W, Wang G. Ligustrazine eases lung cancer by regulating PTEN and Wnt/β-catenin pathway. *Transl Cancer Res*. 2020;9(3):1742–1751. doi:10.21037/tcr.2020.03.26
14. Ma X, Ruan Q, Ji X, Yang J, Peng H. Ligustrazine alleviates cyclophosphamide-induced hepatotoxicity via the inhibition of Txnip/Trx/NF-κB pathway. *Life Sci*. 2021;274:119331. doi:10.1016/j.lfs.2021.119331
15. Zou Y, Zhao D, Yan C, et al. Correction to novel ligustrazine-based analogs of piperlongumine potently suppress proliferation and metastasis of colorectal cancer cells in vitro and in vivo. *J Med Chem*. 2020;63(2):880–881. doi:10.1021/acs.jmedchem.9b02072
16. Qian J, Xu Z, Zhu P, et al. A derivative of piperlongumine and ligustrazine as a potential thioredoxin reductase inhibitor in drug-resistant hepatocellular carcinoma. *J Nat Prod*. 2021;84(12):3161–3168. doi:10.1021/acs.jnatprod.1c00618
17. Liu YL, Yan ZX, Xia Y, et al. Ligustrazine reverts anthracycline chemotherapy resistance of human breast cancer by inhibiting JAK2/STAT3 signaling and decreasing fibrinogen gamma chain (FGG) expression. *Am J Cancer Res*. 2020;10(3):939–952.
18. Gao F, Huang G, Xiao J. Chalcone hybrids as potential anticancer agents: current development, mechanism of action, and structure-activity relationship. *Med Res Rev*. 2020;40(5):2049–2084. doi:10.1002/med.21698
19. Luo Y, Wu W, Zha D, et al. Synthesis and biological evaluation of novel ligustrazine-chalcone derivatives as potential anti-triple negative breast cancer agents. *Bioorg Med Chem Lett*. 2021;47:128230. doi:10.1016/j.bmcl.2021.128230
20. Feng LS, Xu Z, Chang L, et al. Hybrid molecules with potential in vitro antiplasmodial and in vivo antimalarial activity against drug-resistant Plasmodium falciparum. *Med Res Rev*. 2020;40(3):931–971. doi:10.1002/med.21643
21. Li Z, Yulei J, Yaqing J, et al. Protective effects of tetramethylpyrazine analogue Z-11 on cerebral ischemia reperfusion injury. *Eur J Pharmacol*. 2019;844:156–164. doi:10.1016/j.ejphar.2018.11.031
22. Das A, Prajapati A, Karna A, et al. Structure-based virtual screening of chemical libraries as potential MELK inhibitors and their therapeutic evaluation against breast cancer. *Chem Biol Interact*. 2023;376:110443. doi:10.1016/j.cbi.2023.110443
23. Ye J, Deng W, Zhong Y, et al. MELK predicts poor prognosis and promotes metastasis in esophageal squamous cell carcinoma via activating the NF-κB pathway. *Int J Oncol*. 2022;61(2):1–5.
24. Mahasenan KV, Li C. Novel inhibitor discovery through virtual screening against multiple protein conformations generated via ligand-directed modeling: a maternal embryonic leucine zipper kinase example. *J Chem Inf Model*. 2012;52(5):1345–1355. doi:10.1021/ci300040c
25. Yang H, Zhou H, Wang G, et al. MELK is a prognostic biomarker and correlated with immune infiltration in glioma. *Front Neurol*. 2022;13:977180. doi:10.3389/fneur.2022.977180
26. Tang BF, Yan RC, Wang SW, Zeng ZC, Du SS. Maternal embryonic leucine zipper kinase in tumor cells and tumor microenvironment: an emerging player and promising therapeutic opportunity. *Cancer Lett*. 2023;560:216126. doi:10.1016/j.canlet.2023.216126
27. Wang Z, Castro N, Bernstein AM, Wolosin JM. TGFβ1-driven SMAD2/3 phosphorylation and myofibroblast emergence are fully dependent on the TGFβ1 pre-activation of MAPKs and controlled by maternal leucine zipper kinase. *Cell Signal*. 2024;113:110963. doi:10.1016/j.cellsig.2023.110963
28. Nakano I, Paucar AA, Bajpai R, et al. Maternal embryonic leucine zipper kinase (MELK) regulates multipotent neural progenitor proliferation. *J Cell Biol*. 2005;170(3):413–427. doi:10.1083/jcb.200412115
29. Hu Z, Li L, Li M, et al. miR-21-5p inhibits ferroptosis in hepatocellular carcinoma cells by regulating the AKT/mTOR signaling pathway through MELK. *J Immunol Res*. 2023;2023:8929525. doi:10.1155/2023/8929525
30. Tang Q, Li W, Zheng X, et al. MELK is an oncogenic kinase essential for metastasis, mitotic progression, and programmed death in lung carcinoma. *Signal Transduct Target Ther*. 2020;5(1):279. doi:10.1038/s41392-020-00288-3
31. Shannon P, Markiel A, Ozier O, et al. Cytoscape: a software environment for integrated models of biomolecular interaction networks. *Genome Res*. 2003;13(11):2498–2504. doi:10.1101/gr.1239303

32. Chin CH, Chen SH, Wu HH, Ho CW, Ko MT, Lin CY. cytoHubba: identifying hub objects and sub-networks from complex interactome. *BMC Syst Biol*. 2014;8(Suppl 4):S11. doi:10.1186/1752-0509-8-s4-s11

33. Dong D, Xu Z, Zhong W, Peng S. Parallelization of molecular docking: a review. *Curr Top Med Chem*. 2018;18(12):1015–1028. doi:10.2174/1568026618666180821145215

34. Guney E, Menche J, Vidal M, Barábasi AL. Network-based in silico drug efficacy screening. *Nat Commun*. 2016;7:10331. doi:10.1038/ncomms10331

35. Vodenkova S, Buchler T, Cervena K, Veskrnova V, Vodicka P, Vymetalkova V. 5-fluorouracil and other fluoropyrimidines in colorectal cancer: past, present and future. *Pharmacol Ther*. 2020;206:107447. doi:10.1016/j.pharmthera.2019.107447

36. Jiang R, Xu J, Zhang Y, et al. Ligustrazine alleviates psoriasis-like inflammation through inhibiting TRAF6/c-JUN/NFκB signaling pathway in keratinocyte. *Biomed Pharmacother*. 2022;150:113010. doi:10.1016/j.biopha.2022.113010

37. Huang HH, Liu FB, Ruan Z, Zheng J, Su YJ, Wang J. Tetramethylpyrazine (TMPZ) triggers S-phase arrest and mitochondria-dependent apoptosis in lung cancer cells. *Neoplasma*. 2018;65(3):367–375. doi:10.4149/neo_2018_170112N26

38. Yang S, Wu S, Dai W, et al. Tetramethylpyrazine: a review of its antitumor potential and mechanisms. *Front Pharmacol*. 2021;12:764331. doi:10.3389/fphar.2021.764331

39. Lu HY, Zu YX, Jiang XW, et al. Novel ADAM-17 inhibitor ZLDI-8 inhibits the proliferation and metastasis of chemo-resistant non-small-cell lung cancer by reversing Notch and epithelial mesenchymal transition in vitro and in vivo. *Pharmacol Res*. 2019;148:104406. doi:10.1016/j.phrs.2019.104406

40. Gielecińska A, Kciuk M, Yahya EB, Ainane T, Mujwar S, Kontek R. Apoptosis, necroptosis, and pyroptosis as alternative cell death pathways induced by chemotherapeutic agents? *Biochim Biophys Acta Rev Cancer*. 2023;1878(6):189024. doi:10.1016/j.bbcan.2023.189024

41. Wang H, Zhang W, Cheng Y, et al. Design, synthesis and biological evaluation of ligustrazine-flavonoid derivatives as potential anti-tumor agents. *Molecules*. 2018;23(9):2187.

42. Moradipour A, Dariushnejad H, Ahmadizadeh C, Lashgarian HE. Dietary flavonoid carvacrol triggers the apoptosis of human breast cancer MCF-7 cells via the p53/Bax/Bcl-2 axis. *Med Oncol*. 2022;40(1):46. doi:10.1007/s12032-022-01918-2

43. Kramer N, Walzl A, Unger C, et al. In vitro cell migration and invasion assays. *Mutat Res*. 2013;752(1):10–24. doi:10.1016/j.mrrev.2012.08.001

44. Rajasinghe LD, Pindiprolu RH, Gupta SV. Delta-tocotrienol inhibits non-small-cell lung cancer cell invasion via the inhibition of NF-κB, uPA activator, and MMP-9. *Onco Targets Ther*. 2018;11:4301–4314. doi:10.2147/ott.S160163

45. Eberhardt J, Santos-Martins D, Tillack AF, Forli S. AutoDock Vina 1.2.0: new docking methods, expanded force field, and python bindings. *J Chem Inf Model*. 2021;61(8):3891–3898. doi:10.1021/acs.jcim.1c00203

46. Badouel C, Chartrain I, Blot J, Tassan JP. Maternal embryonic leucine zipper kinase is stabilized in mitosis by phosphorylation and is partially degraded upon mitotic exit. *Exp Cell Res*. 2010;316(13):2166–2173. doi:10.1016/j.yexcr.2010.04.019

47. Janostiak R, Rauniyar N, Lam TT, et al. MELK promotes melanoma growth by stimulating the NF-κB pathway. *Cell Rep*. 2017;21(10):2829–2841. doi:10.1016/j.celrep.2017.11.033

48. Xu Q, Ge Q, Zhou Y, et al. MELK promotes Endometrial carcinoma progression via activating mTOR signaling pathway. *EBioMedicine*. 2020;51:102609. doi:10.1016/j.ebiom.2019.102609